Nanosecond-Pulsed Discharge Plasma Splitting of Carbon Dioxide

Moon Soo Bak, Seong-Kyun Im, and Mark Cappelli

***Abstract*— This paper reports on the study of repetitive nanosecond-pulsed discharge splitting of carbon dioxide (CO_2) for the production of CO. Gas chromatography is used to analyze the composition of the reformed gas when CO_2 is exposed to high-voltage (15 kV) very short (10 ns) electrical discharges that deposit as much as 0.4 mJ of energy at a rate of 30 kHz. Conversion rate and energy efficiency are obtained while the discharge pressure is varied between 2.4 and 5.1 atm. At the tested conditions, the maximum conversion rate and energy efficiency are found to be 7.3% and 11.5%, respectively. The energy efficiency drops slightly with increased pressure because of the decreased electric field and electron energy per molecule. An energy balance analysis of a set of CO_2 plasma reactions reveals that the dominant dissociation pathway under these conditions passes through the excitation of CO_2 (10.5 eV) followed by autodissociation into CO and O, which are often in excited states.**

***Index Terms*— Plasma applications.**

I. Introduction

CARBON dioxide (CO_2) produced as a result of the combustion of hydrocarbons in air has been designated as a major species that contributes to global warming. In addition to increasing efforts aimed at improving the thermal efficiency of current combustion systems, two strategies have been proposed to reduce the atmospheric levels of CO_2. One is the capture and sequestration of CO_2 [1] and the other is the conversion of CO_2 into a valued-added product, CO [2]–[13]. Since the CO_2 dissociation reactions

$$\begin{aligned} CO_2 &\rightarrow CO + O \\ \Delta H &= 532 \text{ kJ/mol} = 5.49 \text{ eV/molecule at 300 K} \\ CO_2 &\rightarrow CO + \frac{1}{2} O_2 \\ \Delta H &= 283 \text{ kJ/mol} = 2.92 \text{ eV/molecule at 300 K} \end{aligned} \quad (1)$$

are strongly endothermic with a high activation energy barrier, thermal dissociation requires temperatures between 3300 and 3800 K for the highest theoretical efficiency of 43% [3]. Therefore, catalytic dissociation has been studied based on the use of electrocatalysts [2] and plasma sources [3]–[13] to lower the overall energy barrier and increase the energy efficiency.

Lebouvier *et al.* [3] provided an extensive review of previous results of plasma dissociation of CO_2. The types of plasmas studied include dielectric barrier discharge (DBD) [4], radio frequency (RF) [5], microwave [6], [7], glow [8], gliding arc [9], and corona [10], [11] discharges. The energy efficiency, defined as the ratio of chemical energy output to plasma energy input, has been shown to depend on the average electron energy and its distribution function [3]–[13]. Fridman [12] suggested that the energy efficiency can be as high as 61% through the accumulative excitation of vibrational states, which results in formation of electronically excited $CO_2(^3B_2,v)$ and its autodissociation into ground states of CO and O

$$CO_2(v) \rightarrow CO_2(^3B_2, v) \rightarrow CO + O \quad (2)$$

as well as the secondary reaction between the produced atomic oxygen and excited CO_2

$$\begin{aligned} O + CO_2(v) &\rightarrow CO + O_2 \\ \Delta H &= 33.789 \text{ kJ/mol} = 0.35 \text{ eV/molecule at 300 K.} \end{aligned} \quad (3)$$

Nonthermal plasmas that can selectively populate vibrational and electronic states without raising translational temperature are, therefore, expected to provide a higher CO_2 energy efficiency. The highest energy efficiencies (56% and 37%) were reported for corona [10], [11] and nonequilibrium gliding arc [9] discharges, respectively, whereas relatively low efficiencies (<4% and <3%) were reported for DBD [4] and low-pressure RF discharges [5]. A large difference in energy efficiency has been observed in prior studies even with the use of the same plasma type, and this may be because of the difference in the range of electron energy that each plasma source produces. Simulations carried out of CO_2 splitting by a DBD [13] confirm that vibrational excitation may contribute to the conversion process. Although the results of those simulations indicate that most of the conversion is driven by direct electron-impact dissociation (which explains the relatively low-energy efficiency seen experimentally), the simulations did suggest that the effect of exciting CO_2 vibrational states may be significant when the discharge operating frequencies are high enough to build up vibrational state populations.

Manuscript received January 5, 2015; revised February 6, 2015; accepted February 19, 2015. Date of publication March 10, 2015; date of current version April 13, 2015. This work was supported by the Global Climate and Energy Project through Stanford University, Stanford, CA, USA.

M. S. Bak was with Stanford University, Stanford, CA 94305 USA. He is now with the School of Mechanical Engineering, Sungkyunkwan University, Suwon 440-746, Korea (e-mail: moonsoo@skku.edu).

S.-K. Im was with Stanford University, Stanford, CA 94305 USA. He is now with the Aerospace Engineering Program, Department of Mechanical Engineering, Worcester Polytechnic Institute, Worcester, MA 01609 USA (e-mail: sim@wpi.edu).

M. Cappelli is with the Department of Mechanical Engineering, Stanford University, Stanford, CA 94305 USA (e-mail: cap@stanford.edu).

Color versions of one or more of the figures in this paper are available online at http://ieeexplore.ieee.org.

Digital Object Identifier 10.1109/TPS.2015.2408344

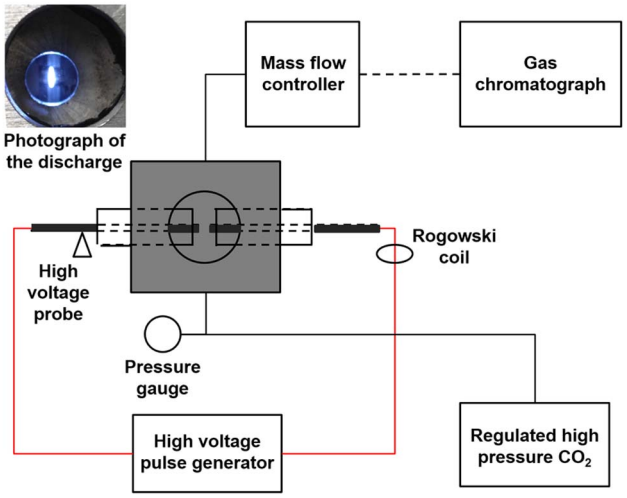

Fig. 1. Experimental setup of nanosecond-pulsed discharge splitting of CO_2 to CO and O_2. Inset: photograph of the discharge.

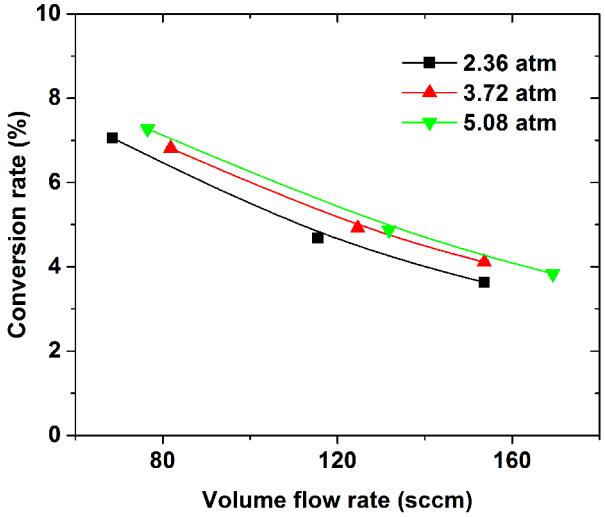

Fig. 2. Conversion rate of CO_2 splitting by repetitive nanosecond-pulsed discharges. The discharge pressure is varied between 2.4 and 5.1 atm, and the volume flow rate is varied from 68.5 to 169 sccm.

In this paper, a repetitive nanosecond-pulsed discharge is used as nonequilibrium plasma source. It has been shown that the peak plasma density in these discharges can be very high ($\sim 10^{15}$ cm^{-3}) with a relatively low power budget when applying a high voltage in a very short duration [14]. In most cases, the plasma is in a highly nonequilibrium state as a result of the relatively long excited state relaxation timescales. These nonequilibrium nanosecond discharge plasmas have been used in stabilizing combustion [15], [16] and in aerodynamic flow control [17]. Here, we examine the effectiveness of such discharges in CO_2 dissociation. We have measured the CO_2 conversion rate and its energy efficiency. The results are then compared with those of previous studies that use other plasma discharges. A few prior studies investigate the dependence of these efficiencies on pressure. Here, we vary the reaction pressure between 2.4 and 5.1 atm. An analysis of energy balance is also carried out on a set of the plasma reactions to determine relevant reaction pathways to CO production.

II. Experimental Setup

A schematic of the experimental setup is shown in Fig. 1. The discharge is generated between the flat ends of two 2.54-mm diameter nickel alloy electrodes separated by 0.7 mm. The electrodes are prepared from conventional automobile spark plugs (NGK spark plugs) after removing the ground tips. The each electrode is driven positively and negatively by a high-voltage pulse generator (FID technology F1112). The net voltage pulse applied between the electrodes has a 16-kV peak voltage and 9.5-ns pulse width. The discharge repetition rate is fixed at 30 KHz while the discharge pressure is varied between 2.4 and 5.1 atm. The working pressure is limited to this range since the discharge either turned into a streamer at lower pressures or extinguished at higher pressures. A photograph of the discharge is also shown in the inset of Fig. 1. The discharge appears to fill the electrode spacing and looks diffuse. During the experiments, the volumetric flow rate of CO_2 varies between 68.5 and 169 sccm using a mass flow controller (MFC) (Tylan FC-260F). The flow rate is also monitored by a flow meter (Matheson E601) at the exit of the MFC because strong electromagnetic interferences generated by the high-voltage pulse generator and plasma can affect the signal generated by the MFC. The voltage and current are measured by a high-voltage probe (Tektronix P6015A) and current probe (Pearson 2877), respectively, with both recorded on a high-resolution oscilloscope (Tektronix TDS 7104, 1-GHz sampling rate). The voltage and current traces are used to calculate the discharge energy deposited into the flow. The measurements are made close to the ends of the electrodes to have the net applied voltage between the electrodes, and the length of the transmission line is sufficiently long to avoid any effect of voltage/current reflection on the recorded traces.

The reformed gas at the exit of the discharge chamber is collected by a gas sealing bag (Tedlar bag). The collected gas is then injected into a gas chromatograph (Varian, Inc.) for the analysis of gas composition. The gas chromatograph used in this paper is equipped with molsieve 5Å and Porapak Q columns and uses both a thermal conductivity detector (TCD) and a pulsed discharge helium ionization detector (PDHID). Gases (e.g., CO_2, CO, and O_2) are separated while passing through the columns and their coarse concentrations are determined by the TCD (with a resolution of below 1% in mole fraction) and fine concentrations by the PDHID (with a resolution of below 100 ppm in mole fraction).

III. Results

The CO_2 conversion rate is defined as the ratio of the reformed CO volume flow rate (Q_{CO}) to the input CO_2 volume flow rate (Q_{CO_2}), which is expressed as

$$CO_2 \text{ conversion rate} = \frac{Q_{CO}}{Q_{CO_2}}. \tag{4}$$

The CO_2 conversion rate obtained using the nanosecond-pulsed discharge at different pressures and volume flow rates

is shown in Fig. 2. Measurements at each condition were conducted three times, and the error ranges in the graph are smaller than the size of symbol. The conversion rate is found to be higher for lower CO_2 volume flow rate. This is expected because more CO_2 molecules will experience plasma reactions as the flow rate decreases at the given discharge conditions. For increased discharge pressures, the conversion rate is found to be slightly higher. A maximum conversion rate of 7.3% is obtained over the range of conditions studied.

A. Nanosecond-Pulsed Discharge Energy Calculation

The energy efficiency η is defined as the ratio of the dissociation enthalpy for CO ($\Delta H_R = 2.92$ eV/molecule as the flow exits at 300 K) to an actual energy cost for the production of one CO molecule in the plasma system (E_{CO}), which is expressed as

$$\eta(\%) = \frac{\Delta H_R(\mathrm{kJ/mol})}{E_{\mathrm{CO}}(\mathrm{kJ/mol})} \times 100. \tag{5}$$

For a given flow rate and plasma power, a specific energy input (SEI) is defined as

$$\mathrm{SEI}\left(\frac{\mathrm{J}}{\mathrm{cm}^3}\right) = \frac{\mathrm{Power\ (W)}}{\mathrm{Flow\ rate\ (cm}^3/\mathrm{min)}} \times 60\left(\frac{\mathrm{s}}{\mathrm{min}}\right) \tag{6}$$

and E_{CO} could be calculated using

$$E_{\mathrm{CO}}\left(\frac{\mathrm{kJ}}{\mathrm{mol}}\right) = \mathrm{SEI}\left(\frac{\mathrm{kJ}}{\mathrm{L}}\right) \times \left[\mathrm{molar\ volume}\ \left(\frac{\mathrm{L}}{\mathrm{mol}}\right)\right] \tag{7}$$

for different discharge pressures.

Therefore, the measurement of a discharge energy that is deposited into the flow is required to determine the energy efficiency of the splitting process. Here, we calculate the discharge energy during a pulse (E_{pulse}) by integrating the product of the discharge voltage and the current (I) over the pulse interval (τ)

$$E_{\mathrm{pulse}} = \int_0^{\tau} V(t)I(t)dt. \tag{8}$$

As mentioned, the measurements are carried out very close to the electrode ends and the signal lines of the both probes have the same lengths. However, determining a right timing between the two measurements are still important since these voltage and current change within a few nanoseconds. In this paper, voltage and current are recorded not only in the presence of the plasma but also in the absence of the plasma. Without forming a plasma, the current represents mostly a displacement current ($I_{\mathrm{displacement}}$) and the exact timing could be found by matching that measured and calculated using

$$I_{\mathrm{displacement}} = C_{\mathrm{eff}}\frac{dV}{dt}. \tag{9}$$

Fig. 3 shows the time-averaged voltage and both measured and calculated displacement currents at 3.7-atm pressure when the discharge formation is suppressed. Without a discharge, the effective capacitance of the circuit (C_{eff}) is found to be 4.65 nF.

The time-averaged voltage and current curves when the discharge is produced are shown in Fig. 4. We see that the current peaks at about 24 A immediately after the voltage

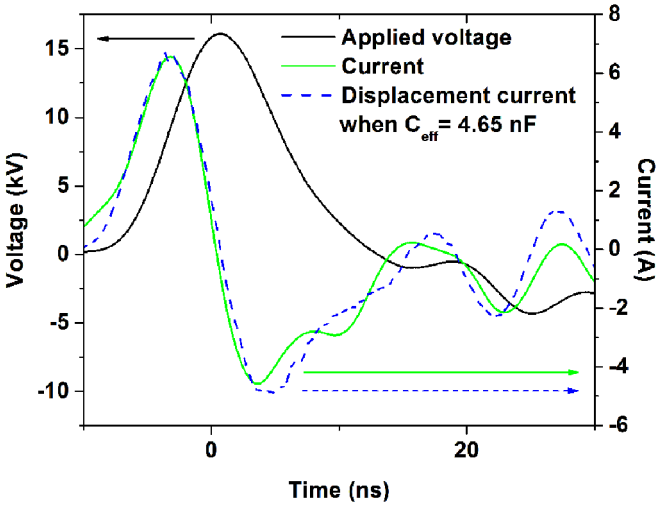

Fig. 3. Typical voltage and current curves when the plasma is not produced. The solid black line represents the voltage near the electrodes, whereas the solid green and dashed blue lines represent the measured and calculated displacement currents, respectively.

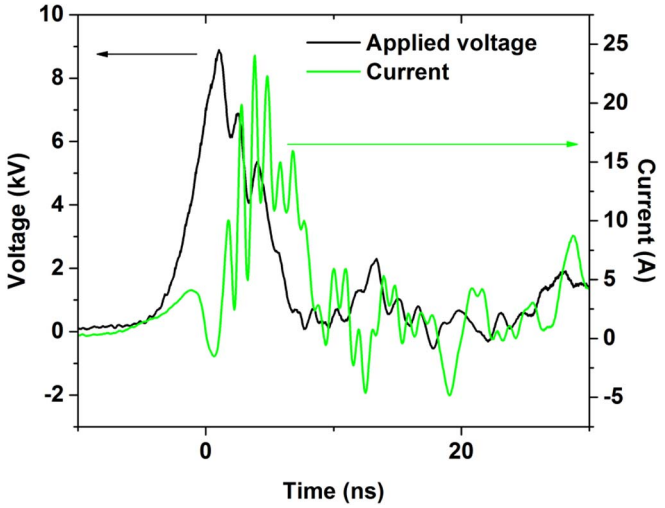

Fig. 4. Typical voltage and current curves when the plasma is produced at a pressure of 3.72 atm and a volume flow rate of 82 sccm. The solid black line represents the voltage near the electrodes, whereas the solid green line represents the total current.

undergoes a significant drop. This voltage drop appears well before the voltage reaches its peak in the absence of a discharge (Fig. 3), and it is often seen in a glow-to-arc transition where the current determines the maximal voltage and power.

The plasma energy calculation was conducted several times for each condition to check on reproducibility and the difference between several measurements was found to be less than 2%. The energy deposited by the discharge into the CO_2 is found to increase from 308 to 358 μJ, and then to 381 μJ as the discharge pressure increases from 2.4 to 3.7 atm, and finally to 5.1 atm, respectively. This energy is almost independent of the volume flow rate. Since a direct-current power supply delivered 21 W to the pulser under the tested pressures, the device efficiency ranges between 44% and 54%

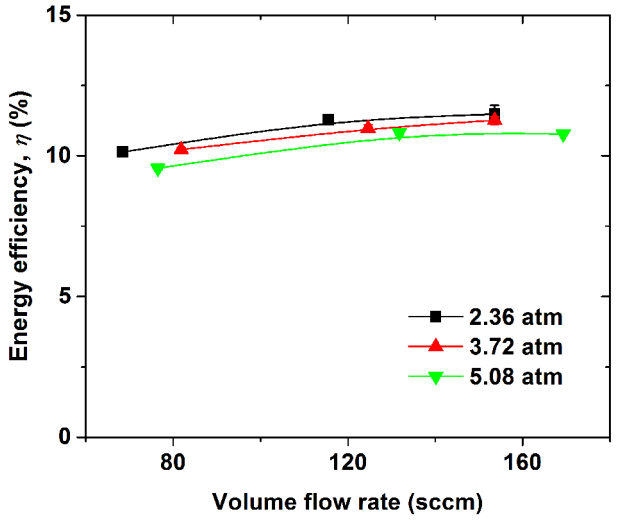

Fig. 5. Energy efficiency of CO_2 splitting by repetitive nanosecond-pulsed discharges. The discharge pressure is varied between 2.4 and 5.1 atm, and the volume flow rate is varied from 68.5 to 169 sccm.

and this is somewhat lower than that of the manufacture specification (i.e., 70% given at 50–100-Ω load). The results shows that the energy coupling between the plasma and the gas between the electrodes (e.g., CO_2 and a fraction of its dissociated products) is better at the higher pressures, and this might result from better impedance matching between the plasma and pulser circuit. This higher energy coupling for the higher pressures turns out to be responsible for the observed increase in conversion rate at higher pressures.

B. Energy Efficiency of Discharge Splitting of CO_2

The energy efficiency (η) of the CO_2 splitting process for varying pressure and volume flow rate is shown in Fig. 5. These measurements are obtained from the measured conversion rate and calculated plasma deposited energy discussed above. The energy efficiency is found to increase slightly with increased volume flow rate, but decrease slightly with increasing discharge pressure. The trend for increased pressures is opposite to that of the conversion rate, which was found to be higher at higher pressure. This implies that although energy coupling between the plasma and the pulser circuit is better at higher pressures, plasma reactions leading to CO_2 dissociation become less energy efficient. Since the reduced electric field (E/N) is expected to be lower for higher pressures, the decreased efficiency is attributed to the decreased electron energy per molecule. As we are in an E/N regime that favors electronic excitation (discussed below), excited states of CO_2 that have lower threshold energies than that to break the CO = O bond (e.g., 8.3 eV) will be more favorably populated at these high pressures and eventually result in a decrease in energy efficiency.

C. Energy Balance Analysis of CO_2 Plasma Reactions

An analysis of the energy balance is carried out on a set of plasma reactions that may be important in the CO_2 splitting process. In the plasma, the imposed electric field is mostly coupled to the translational motion of the electrons because of the electrons' relatively higher mobility than that of ions. The energetic electrons then transfer their energy to heavy particles, e.g., CO_2, through inelastic electron-impact collisions. The resulting excited and ionized states are subsequently quenched and recombined with electrons. Some of these reactions break the CO = O bond, forming CO. The inelastic electron-impact reactions considered in this paper are listed below and the cross sections are taken from the compilation in [18]

$$\text{R1}: e + CO_2 \rightarrow CO + O^-$$
$$\text{R2}: e + CO_2 \rightarrow e + CO_2(v,\ \text{sum of all vibrational states})$$
$$\text{R3}: e + CO_2 \rightarrow e + CO_2(2.5\ \text{eV})$$
$$\text{R4}: e + CO_2 \rightarrow e + CO_2(7\ \text{eV})$$
$$\text{R5}: e + CO_2 \rightarrow e + CO_2(10.5\ \text{eV})$$
$$\text{R6}: e + CO_2 \rightarrow 2e + CO_2^+(13.8\ \text{eV}).$$

These reactions include the dissociative attachment of electrons (R1), excitation of vibrational (R2) and various electronic states (R3-5), and ionization of CO_2 (R6). We note that these electronic states are not specific but, rather, are lumped along with their nearby states. Although the electron attachment reaction is the only direct pathway in forming CO, it is known that other states can also contribute to the CO formation.

In this analysis, we estimate the fraction of the overall energy efficiency that each plasma reaction and its ensuing reactions accounts for. The amount of each reaction pathway that contributes to the total energy efficiency will be the product of the energy loss fraction of an electron-impact reaction (e.g., R1-6) and the fraction of its deposited energy recovered into a chemical form of CO (which we call energy recovery fraction). The energy loss fractions associated with electron-impact reactions are computed as a function of the reduced electric field (E/N) using the *BOLSIG+* software package [19]. The results are shown in Fig. 6. Under the studied discharge conditions, the reduced electric field corresponding to a maximum current is determined to range between 90 and 135 Td based on (10) and (11) and the measured breakdown voltage. When the plasma conducts a large amount of current, E/N is reduced to a value where the growth rate of the plasma is in a similar order of magnitude as its decay rate. It is described as

$$\frac{k_{\text{ioniz}} n_e N}{k_{\text{recomb}} n_e n_{CO_2^+} + k_{\text{att}} n_e N} \approx 1 - 10, \quad n_e \approx n_{CO_2^+} \tag{10}$$

and

$$I_{\text{conduction}} \approx e n_e \mu_e E A_d. \tag{11}$$

In the equations, k_{ioniz}, k_{recomb}, and k_{att} are the ionization, electron–ion recombination, and electron attachment reaction coefficients, respectively, and μ_e is the electron mobility. These values are also obtainable from the *BOLSIG+* calculation as a function of E/N. n_e and n_{CO_2+} are the number densities of electron and CO_2^+ ion, N is the total number density, $I_{\text{conduction}}$ is the conduction current, E is the electric field (given as the measured voltage divided by the electrode spacing), and A_d is the cross-sectional area of the discharge.

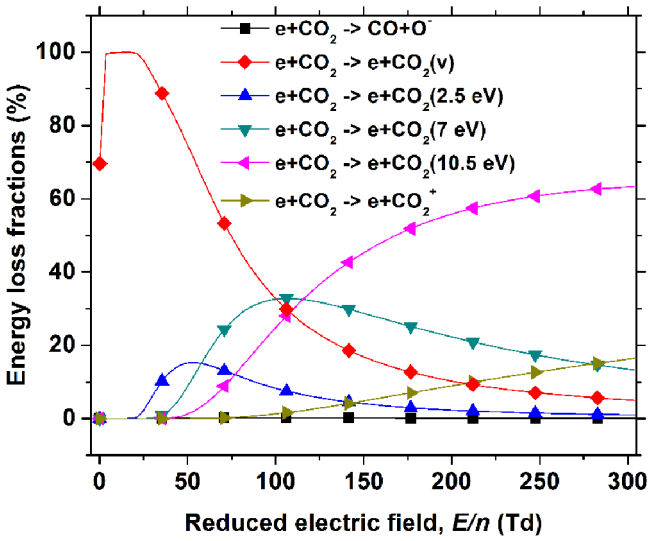

Fig. 6. Energy loss fractions by each inelastic electron-impact reactions of CO_2. The reactions include electron-attachment, electron-impact excitation of vibrational and electronic states, and ionization.

From Fig. 6, most of the plasma energy is coupled to vibration excitation of CO_2 (v) and electronic excitation of CO_2 (7 eV) and CO_2 (10.5 eV). The role of CO_2 (10.5 eV) is expected to be significant because of its energy being higher than that of the CO = O bond (e.g., 8.3 eV). However, those of CO_2 (v) and CO_2 (7 eV) have lesser contributions as they require stepwise excitation to higher energy states within a short pulse duration and at relatively low discharge repetition rates.

The energy recovery fraction for each electron-impact reaction resulting in the formation of CO depends on the ensuing reactions. It is clearer for electron attachment (R1), excitation of CO_2 (10.5 eV) (R5), and ionization of CO_2^+ (13.8 eV) (R6) since their fates are mainly dissociative attachment, autodissociation (R7), and dissociative recombination (R8)

$$\mathrm{R7}: \mathrm{CO_2}(10.5\ \mathrm{eV}) \rightarrow \mathrm{CO} + \mathrm{O}$$
$$\mathrm{R8}: e + \mathrm{CO_2^+}(13.8\ \mathrm{eV}) \rightarrow \mathrm{CO} + \mathrm{O}.$$

Therefore, the energy recovery fractions of R1, R5, and R6 are 100%, 27.8% (i.e., an energy of 2.92 eV stored in CO at given deposited electron energy of 10.5 eV), and 21.2% (i.e., 2.92/13.8 eV), respectively. Given the range of the reduced electric field, the energy efficiencies that R1, R5, and R6 result in are estimated to be 0.18%–0.21%, 5.7%–11.5%, and 0.18%–0.81%, respectively. We find that the excitation and autodissociation pathways of CO_2 (10.5 eV) are responsible for the majority of the measured energy efficiency (e.g., 9.6%–11.5%) although the obtained range is rather broad. The contribution from step-wise excitations of energy states lower than 10.5 eV (2) seems to be less significant in forming CO. These results are mainly because the range of the reduced electric field under the studied discharge conditions favor electronic excitation. Our findings are consistent with previous simulation results of CO_2 splitting with DBDs [13], where most of the CO_2 dissociation is attributed to direct electron-impact process and a significant contribution of vibrational states to CO_2 dissociation is expected at frequencies higher than 1 MHz.

The measured energy efficiency of 11.5% for this nanosecond-pulsed discharge reforming process is higher than that measured for DBD (<4%) [4] and low-pressure RF discharges (<3%) [5], but lower than that reported using corona discharges (56%) [10], [11] and nonequilibrium gliding arc discharges (37%) [9]. Our lower energy efficiency may be a result of the relatively high average electron energy produced at these high values of E/N. These higher energies are not optimized for the vibrational excitation–dissociation pathway described by (2). Furthermore, the discharge repetition rate may be too low to build up the vibrational state populations before subsequent quenching of these states. Future work will move toward operation at higher frequencies and toward extending the range of E/N to both higher and lower values.

IV. Conclusion

This research involved the study of nanosecond-pulsed repetitive discharge splitting of CO_2 to produce CO and O_2. The effectiveness of the process was characterized by gas chromatography. At the tested discharge conditions, it was found that more energy was coupled into the plasma as the reactor pressure increased from 2.4 to 5.1 atm. The conversion rate was also found to be higher for increased reactor pressure. However, the energy efficiency of the CO_2 splitting was lower for increased pressure. This may be because of the decreased electric field and electron energy per molecule at higher pressures. From the energy balance analysis of the plasma reactions, the excitation and autodissociation of CO_2 (10.5 eV) is suggested to be the dominant reaction pathway to the formation of CO.

References

[1] C. M. White, B. R. Strazisar, E. J. Granite, J. S. Hoffman, and H. W. Pennline, "Separation and capture of CO_2 from large stationary sources and sequestration in geological formations—Coalbeds and deep saline aquifers," *J. Air Waste Manage. Assoc.*, vol. 53, no. 6, pp. 645–715, Jun. 2003.

[2] Z. Chen *et al.*, "Splitting CO_2 into CO and O_2 by a single catalyst," *Proc. Nat. Acad. Sci. United States Amer.*, vol. 109, no. 39, pp. 15606–15611, Sep. 2012.

[3] A. Lebouvier, S. A. Iwarere, P. d'Argenlieu, D. Ramjugernath, and L. Fulcheri, "Assessment of carbon dioxide dissociation as a new route for syngas production: A comparative review and potential of plasma-based technologies," *Energy Fuels*, vol. 27, no. 5, pp. 2712–2722, 2013.

[4] S. Paulussen *et al.*, "Conversion of carbon dioxide to value-added chemicals in atmospheric pressure dielectric barrier discharges," *Plasma Sour. Sci. Technol.*, vol. 19, no. 3, pp. 034015-1–034015-6, May 2010.

[5] L. F. Spencer and A. D. Gallimore, "Efficiency of CO_2 dissociation in a radio-frequency discharge," *Plasma Chem. Plasma Process.*, vol. 31, no. 1, pp. 79–89, Feb. 2011.

[6] A. Vesel, M. Mozetic, A. Drenik, and M. Balat-Pichelin, "Dissociation of CO_2 molecules in microwave plasma," *Chem. Phys.*, vol. 382, nos. 1–3, pp. 127–131, Apr. 2011.

[7] M. Tsuji, T. Tanoue, K. Nakano, and Y. Nishimura, "Decomposition of CO_2 into CO and O in a microwave-excited discharge flow of CO_2/He or CO_2/Ar mixtures," *Chem. Lett.*, vol. 30, no. 1, pp. 22–23, 2001.

[8] J.-Y. Wang, G.-G. Xia, A. Huang, S. L. Suib, Y. Hayashi, and H. Matsumoto, "CO_2 decomposition using glow discharge plasmas," *J. Catalysis*, vol. 185, no. 1, pp. 152–159, Jul. 1999.

[9] T. Nunnally, K. Gutsol, A. Rabinovich, A. Fridman, A. Gutsol, and A. Kemoun, "Dissociation of CO_2 in a low current gliding arc plasmatron," *J. Phys. D, Appl. Phys.*, vol. 44, no. 27, pp. 274009-1–274009-7, Jul. 2011.

[10] T. Mikoviny, M. Kocan, S. Matejcik, N. J. Mason, and J. D. Skalny, "Experimental study of negative corona discharge in pure carbon dioxide and its mixtures with oxygen," *J. Phys. D, Appl. Phys.*, vol. 37, no. 1, pp. 64–73, 2004.
[11] G. Horváth, J. D. Skalny, and N. J. Mason, "FTIR study of decomposition of carbon dioxide in dc corona discharges," *J. Phys. D, Appl. Phys.*, vol. 41, no. 22, pp. 225207-1–225207-8, Nov. 2008.
[12] A. Fridman, *Plasma Chemistry*. New York, NY, USA: Cambridge Univ. Press, 2008.
[13] R. Aerts, T. Martens, and A. Bogaerts, "Influence of vibrational states on CO_2 splitting by dielectric barrier discharges," *J. Phys. Chem. C*, vol. 116, no. 44, pp. 23257–23273, 2012.
[14] D. Z. Pai, D. A. Lacoste, and C. O. Laux, "Nanosecond repetitively pulsed discharges in air at atmospheric pressure—The spark regime," *Plasma Sour. Sci. Technol.*, vol. 19, no. 6, pp. 065015-1–065015-10, Dec. 2010.
[15] G. Pilla, D. Galley, D. A. Lacoste, F. Lacas, D. Veynante, and C. O. Laux, "Stabilization of a turbulent premixed flame using a nanosecond repetitively pulsed plasma," *IEEE Trans. Plasma Sci.*, vol. 34, no. 6, pp. 2471–2477, Dec. 2006.
[16] M. S. Bak, H. Do, M. G. Mungal, and M. A. Cappelli, "Plasma-assisted stabilization of laminar premixed methane/air flames around the lean flammability limit," *Combustion Flame*, vol. 159, no. 10, pp. 3128–3137, Oct. 2012.
[17] D. V. Roupassov, A. A. Nikipelov, M. M. Nudnova, and A. Y. Starikovskii, "Flow separation control by plasma actuator with nanosecond pulsed-periodic discharge," *AIAA J.*, vol. 47, no. 1, pp. 168–185, Jan. 2009.
[18] A. V. Phelps. *Database*. [Online]. Available: http://www.lxcat.net, accessed May 16, 2014.
[19] G. J. M. Hagelaar. *BOLSIG+: Electron Boltzmann Equation Solver*. [Online]. Available: http://www.bolsig.laplace.univ-tlse.fr, accessed Feb. 4, 2011.

Moon Soo Bak received the B.S. degree in mechanical and aerospace engineering from Seoul National University, Seoul, Korea, in 2007, and the M.S. and Ph.D. degrees in mechanical engineering from Stanford University, Stanford, CA, USA, in 2010 and 2014, respectively.

He is currently a Visiting Professor with the School of Mechanical Engineering, Sungkyunkwan University, Suwon, Korea. His current research interests include combustion, fluid dynamics, atmospheric pressure plasmas, and plasma-assisted combustion.

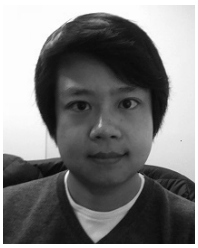

Seong-Kyun Im received the B.S. degree in mechanical and aerospace engineering from Seoul National University, Seoul, Korea, in 2007, and the M.S. and Ph.D. degrees in mechanical engineering from Stanford University, Stanford, CA, USA, in 2009 and 2013, respectively.

He is currently an Assistant Professor with the Aerospace Engineering Program, Department of Mechanical Engineering, Worcester Polytechnic Institute, Worcester, MA, USA. His current research interests include control of subsonic and supersonic aerodynamic flows, compressible flows, plasma-assisted combustion, and supersonic combustion.

Mark Cappelli received the B.A.Sc. degree in physics from McGill University, Montréal, QC, Canada, in 1980, and the M.A.Sc. and Ph.D. degrees in aerospace science and engineering from the University of Toronto, Toronto, ON, Canada, in 1983 and 1987, respectively.

He is currently a Professor with the Department of Mechanical Engineering, Stanford University, Stanford, CA, USA. His current research interests include plasmas and gas discharges, including plasma diagnostics as they apply to aerodynamic and space propulsion, combustion, material processing, fusion, natural phenomenon, and medicine.